BIOCHEMICAL PHARMACOLOGY 74 (2007) 1575–1586

available at www.sciencedirect.com

ScienceDirect

journal homepage: www.elsevier.com/locate/biochempharm

Anti-tumor potential of 15,16-dihydrotanshinone I against breast adenocarcinoma through inducing G1 arrest and apoptosis

Sun-Lung Tsai[a], *Fat-Moon Suk*[b], *Chun-I. Wang*[c], *Der-Zen Liu*[d], *Wen-Chi Hou*[e], *Pei-Jung Lin*[c], *Ling-Fang Hung*[c], *Yu-Chih Liang*[c,f,*]

[a] *Liver Research Unit, Department of Medical Research, Chi-Mei Medical Center, Yung-Kang City, Tainan, Taiwan*
[b] *Department of Internal Medicine, Taipei Medical University Hospital & Wan-Fang Hospital, Taipei, Taiwan*
[c] *School of Medical Laboratory Science & Biotechnology, College of Medicine, Taipei Medical University, Taipei, Taiwan*
[d] *Graduate Institutes of Biomedical Materials, Taipei Medical University, Taipei, Taiwan*
[e] *Graduate Institute of Pharmacognosy Science, College of Pharmacy, Taipei Medical University, Taipei, Taiwan*
[f] *Traditional Herbal Medicine Research Center, Taipei Medical University Hospital, Taipei, Taiwan*

ARTICLE INFO

Article history:
Received 21 June 2007
Accepted 7 August 2007

Keywords:
15,16-Dihydrotanshinone I
Breast cancer
Apoptosis
G1 arrest
Caspase
Cell cycle

ABSTRACT

Chemotherapeutic drugs are usually designed to induce cancer cell death via cell cycle arrest and/or apoptosis pathways. In this study, we used the chemical drug 15,16-dihydrotanshinone I (DHTS) to inhibit breast cancer cell proliferation and tumor growth, and investigate the underlying molecular mechanisms. Human breast cancer cell lines MCF-7 and MDA-MB-231 were both used in this study, and DHTS was found to significantly decrease cell proliferation by a dose-dependent manner in both cells. Flow cytometry indicated that DHTS induced G1 phase arrest in synchronous MCF-7 and MDA-MB-231 cells. When analyzing the expression of cell cycle-related proteins, we found that DHTS reduced cyclin D1, cyclin D3, cyclin E, and CDK4 expression, and increased CDK inhibitor p27 expression in a dose-dependent manner. In addition, DHTS inhibited the kinase activities of CDK2 and CDK4 by an immunocomplex kinase assay. In addition, DHTS also induced apoptosis in both cells through mainly mitochondrial apoptosis pathways. We found that DHTS decreased the anti-apoptotic protein Bcl-xL level and increased the loss of mitochondria membrane potential and the amount of cytochrome *c* released. Moreover, DHTS activated caspase-9, caspase-3, and caspase-7 and caused cell apoptosis. The fact that DHTS-induced apoptosis could be blocked by pretreating cells with pan-caspase inhibitor confirmed that it is mediated through activation of the caspase-3-dependent pathway. In a nude mice xenograft experiment, DHTS significantly inhibited the tumor growth of MDA-MB-231 cells. Taken together, these results suggest that DHTS can inhibit human breast cancer cell proliferation and tumor growth, and might have potential chemotherapeutic applications.

* *Corresponding author at*: School of Medical Laboratory Science & Biotechnology, College of Medicine, Taipei Medical University, No. 250, Wu-Hsing Street, Taipei 11014, Taiwan, ROC. Tel.: +886 2 27361661x3318; fax: +886 2 27393447.
E-mail address: ycliang@tmu.edu.tw (Y.-C. Liang).

Abbreviations: DHTS, 15,16-dihydrotanshinone I; TS, tanshinone I; CTS, cryptotanshinone I; CDK, cyclin-dependent kinase; Bcl-2, B-cell leukemia/lymphoma 2; APAF-1, apoptotic protease activity factor-1; PI, propidium iodide.

0006-2952/$ – see front matter © 2007 Elsevier Inc. All rights reserved.
doi:10.1016/j.bcp.2007.08.009

1. Introduction

Breast cancer is the most common type of tumor in females, and incidence tends to increase with age. Treatment typically involves excision surgery combined with chemotherapy and/or radiation therapy. Recently, an advanced targeted therapy gas was developed and clinically applied [1,2], but it is too expensive to treat more than a handful of patients, and the overall prognosis remains poor. Tumorigenesis encompasses multiple processes involving the dysregulation of a number of molecular pathways, such as cell cycle proliferation, angiogenesis, and apoptosis. The strategy of chemotherapy is based on the use of chemicals able to retard cell cycle progression, inhibit angiogenesis, and induce apoptosis.

Induction of apoptosis has been considered the major cytotoxic mechanism of anticancer therapy. To date, three apoptotic pathways have been addressed, including the mitochondrial pathway [3,4], death receptor pathway [4–6], and endoplasmic reticulum stress-mediated apoptosis pathway [7,8]. The mitochondrial pathway initiates apoptosis in most physiological and pathological situations. The permeabilization of the out mitochondrial membrane plays the most important role in mitochondrial apoptosis. It allows several pro-apoptotic factors, such as cytochrome *c* [9,10] to be released into the cytosol. The B-cell leukemia/lymphoma 2 (Bcl-2) family of pro-apoptotic and anti-apoptotic proteins includes other important regulators of mitochondrial apoptosis [11,12]. Anti-apoptotic proteins Bcl-2 and Bcl-xL prevent mitochondrial apoptosis initiation through interaction with pro-apoptotic protein Bax and/or Bak [13]. The release of cytochrome *c* into cytosol changes the conformation of apoptotic protease activity factor-1 (APAF-1) and activates pro-caspase-9, subsequently activating downstream effector caspases including caspase-3. When activation of caspases cascade, they destroy cellular machinery and lead to eventual cell death [14,15].

15,16-Dihydrotanshinone I (DHTS, Fig. 1A) is a component from the well-known traditional Chinese medicinal plant *Salvia miltiorrhiza* Bunge (Tanshen). It has multiple therapeutic activities and is used to treat vasculocardiac disease, hepatitis, inflammation, and cancer [16,17]. Several bioactive ingredients have been identified in Tanshen, such as water-soluble phenolic acids and lipophilic tanshinones. Previous studies have demonstrated the biological function of DHTS, including liver protective [18] and anti-inflammatory activities [19,20] as well as induced osteoclast differentiation [21] and tumor cells apoptosis [22]. Even though DHTS is effective on human erythroleukemia cell apoptosis, the exact mechanism for treatment of cancer cells is poorly understood. In this study, we found that DHTS was able to induce cell cycle arrest in the G1 phase and apoptosis in human breast adenocarcinoma both in vitro and in vivo.

2. Materials and methods

2.1. Materials

DHTS, TS, and CTS were purchased from Xi'an Honson Biotechnology Co. (Xi'an, China). Their purity was over 90% according to HPLC analysis.

2.2. Cell culture

The human breast adenocarcinoma cell lines MCF-7 (BCRC 60436) and MDA-MB-231 (BCRC 60425) were obtained from Food Industry Research and Development Institute (Hsinchu, Taiwan) and cultured in Dulbecco's modified Eagle medium containing 10% heat-inactivated fetal bovine serum (Biological Industries Ltd., Israel). For all assays, cells were plated in 6-cm dishes at 5×10^6 cells per dish and allowed to grow for 24 h.

2.3. MTT assay

Cells were cultured in a 24-well plate for 24 h and then treated with drugs for another 24 h. When the cell viability had been determined, the medium was removed from each well and another 200 μl of fresh medium as well as 50 μl MTT (2 mg/ml) was added at 37 °C in the dark. After 2 h, the medium was removed, and 200 μl DMSO and 25 μl Sorensen's glycine buffer were added. The supernatant (100 μl) was put into a 96-well plate and the absorbance at OD 570 nm was measured by an ELISA plate reader.

2.4. Extraction of cytosol and mitochondria lysate

Cells were washed with cold PBS twice and homogenized in cytosol extraction buffer (20 mM HEPES pH 7.5, 10 mM KCl, 1.5 mM $MgCl_2$, 1 mM EDTA, 1 mM EGTA, 1 mM DTT, 0.1 mM PMSF, and 250 mM sucrose) for 30 strokes. After centrifugation $700 \times g$ for 10 min at 4 °C to remove the debris, the supernatant was then centrifuged at $10{,}000 \times g$ for 30 min at 4 °C. The supernatant was the cytosol lysate, and the pellet was suspended in Golden protein extraction buffer (137 mM NaCl, 20 mM Tris, pH7.9, 10 mM NaF, 5 mM EDTA, 1 mM EGTA, 10% (v/v) glycerol, 1% Triton X-100, 1 mM sodium orthovanadate, 1 mM sodium pyrophosphate, 100 μM β-glycerophosphate, 1 mM PMSF, 10 μg/ml aprotinin, and 10 μg/ml leupeptin) and centrifugated to obtain the mitochondrial lysate.

2.5. Western blot

Equal amounts of total cellular protein (50 μg) were resolved by 10% SDS-polyacrylamide gel electrophoresis and transferred onto a PVDF membrane (Millipore, Bedford, MA) as described previously [23]. The membrane was then incubated with the following antibodies: anti-PCNA, anti-Rb, anti-phospho-Rb, anti-CDK2, anti-CDK4, anti-CDK6, anti-cyclin D1, anti-cyclin D3, anti-cyclin E, anti-p53, anti-phospho-p53, anti-p15, anti-Bcl-xL, anti-Bcl-2, anti-caspase-3, anti-caspase-7, anti-caspase-9, anti-cytochrome *c* (Cell Signaling Technology Inc., Danvers, MA), anti-p21, and anti-p27 (Santa Cruz Biotechnology, Santa Cruz, CA). The membranes were subsequently incubated with anti-mouse or anti-rabbit IgG antibody conjugated to horseradish peroxidase (Santa Cruz Biotechnology) and visualized using enhanced chemiluminescence kits (Amersham, Arlington, IL).

2.6. CDK kinase activity assay

Equal amounts of total cellular protein (150 μg) were immunoprecipitated with CDK2 or CDK4 antibody (Santa

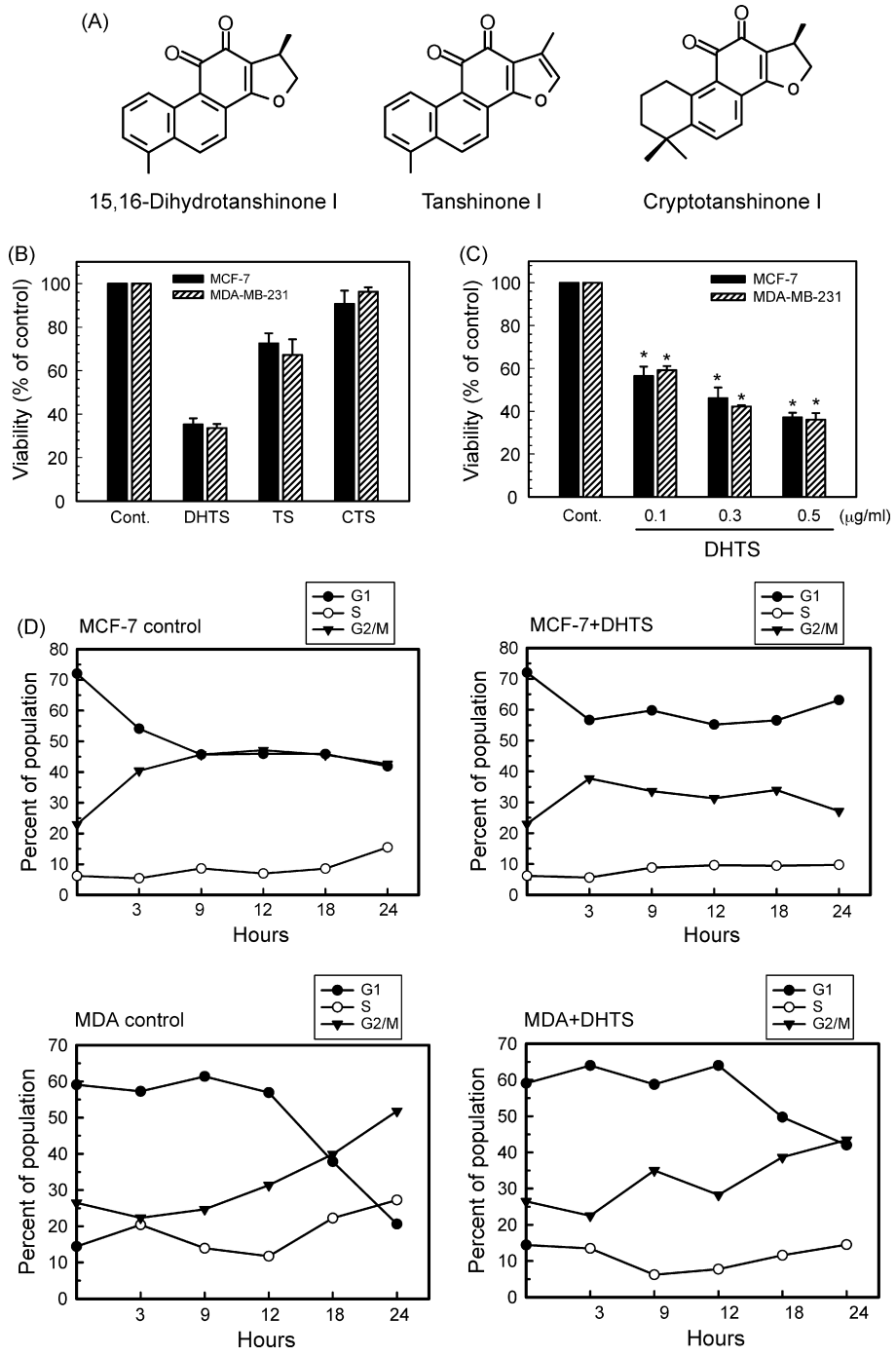

Fig. 1 – Effect of DHTS on the viability and the cell cycle profiles of breast adenocarcinoma cells. (A) Structures of 15,16-dihydrotanshinone I (DHTS), tanshinone I (TS), and cryptotanshinone I (CTS). (B) MCF-7 cells or MDA-MB-231 cells were treated with 0.5 μg/ml of DHTS, TS, or CTS for 24 h, and determined cell viability by MTT assay. (C) MCF-7 cells or MDA-MB-231 cells were treated with 0.1 μg/ml, 0.3 μg/ml, or 0.5 μg/ml of DHTS for 24 h, and cell viability was determined by MTT assay. The values were obtained in three independent experiments performed in triplicate and were represented as means ± S.E. *$p < 0.05$ versus control. (D) MCF-7 cells or MDA-MB-231 cells were treated with 0.5 μg/ml of DHTS for various time points. DNA histogram and the percentages of cells in cell cycle phase were analyzed by flow cytometry.

Cruz Biotechnology) and protein A/G-PLUS agarose for 15 h at 4 °C as described previously [24]. The kinase reactions were carried out in a final volume of 40 μl, containing 1 μg histone H1 (CDK2 substrate) or 2 μg Gst-Rb (CDK4 substrate), 10 μM cold ATP, and 5 μCi [r-32p] ATP (5000 Ci/mmol, Amersham), and the mixture was incubated for 20 min at 25 °C. Each sample was mixed with 10 μl of 5× Laemmli's loading buffer to stop the reaction, heated for 10 min at 100 °C, and subjected to SDS-PAGE. The gels were dried and visualized by autoradiography.

2.7. Flow cytometry analysis for cell cycle distribution

The population of cell cycle was analyzed by flow cytometry as described previously [25]. Briefly, cells were trypsinized, washed twice with PBS, and fixed in 75% ethanol for 1 h at −20 °C. Fixed cells were then washed with PBS, incubated with 0.5 ml PBS containing 0.05% RNase and 0.5% Triton X-100 for 30 min at 37 °C, and stained with propidium iodide (PI). The stained cells were analyzed using a FACscan flow cytometry and FACSVantage SE analysis software (Becton Dickinson, San Jose, CA).

2.8. Flow cytometry analysis for apoptotic cell death

The apoptotic cell death was analyzed by flow cytometry using the Annexin V-conjugated Alexa Fluor488 Apoptosis Detection Kit according the manufacturer's instructions (Molecular Probes, Inc. Eugene, OR). Briefly, cells were trypsinized, washed twice with PBS, and resuspended in annexin-binding buffer (10 mM HEPES, 140 mM NaCl, and 2.5 mM $CaCl_2$, pH 7.4) to $\sim 1 \times 10^5$ cells/100 μl. The cells were stained with 5 μl Annexin V-Alexa Fluor 488 and PI (1 μg/ml) at room temperature for 15 min in the dark. The stained cells were analyzed by FACScan flow cytometry using CellQuest 3.3 analysis software (Becton Dickinson).

2.9. Mitochondrial membrane potential analysis

The loss of mitochondrial membrane potential was quantitatively determined by flow cytometry using the MitoProbe™ JC-1 Assay Kit according the manufacturer's instructions (Molecular Probes). Briefly, cells were trypsinized, washed twice with warm PBS, and resuspended in warm PBS to $\sim 1 \times 10^6$ cells/1 ml. The cells were then stained with 10 μl of 200 μM JC-1 dye at 37 °C for 30 min in the dark and analyzed immediately by FACScan flow cytometry using CellQuest 3.3 analysis software (Becton Dickinson).

2.10. Caspase-3 activity assay

Briefly, cells were washed with cold PBS twice, and the cytosolic fraction was extracted with extraction buffer as described previously [24]. Cell lysate (150 μg) was incubated with 30 μM fluorescence substrate, acetyl-Asp-Glu-Val-Asp-7-amido-4-methylcoumarin (Ac-DEVD-AMC, BIOMOL International, L.P., Plymouth Meeting, PA) in assay buffer (50 mM HEPES, pH 7.4, 100 mM NaCl, 0.1% CHAPS, 10 mM DTT, 1 mM EDTA, 10% glycerol) at 37 °C for 1 h in the dark. The fluorescence intensity of the cleaved substrate was measured on a Plate Chameleon Multilabel plate reader (HIDEX OY, Turku, Finland) by Ex 340 nm/Em 460 nm.

2.11. Transition transfection assays

For luciferase reporter assay, cells were seeded in 24-well plates. The next day, the cells were replaced the serum-free Opti-MEM (Invitrogen Corporation, Carlsbad, CA) and transfected with the cyclin D1 promoter luciferase reporter plasmids [26] and phRL-TK (Promega, Madison, WI) as an internal control plasmid using LipofectAMINE2000™ (Invitrogen). After 36 h of transfection, the cells were treated with various concentrations of DHTS for 18 h and harvested cell lysate in 100 μl of assay buffer (0.5 M Hepes pH 7.8, 1% Triton N-101, 1 mM $CaCl_2$, and 1 mM $MgCl_2$). Luciferase activities were determined by RenLite™ luciferase reporter gene assay kit (Packard Instrument Company, Meriden, CT) and Plate Chameleon Multilabel plate reader (HIDEX).

2.12. Anti-tumor nude mice experiment

Male Balb/cAnN-Foxn1 nude mice (4–5 weeks old) were purchased from the National Laboratory Animal Center (Taipei, Taiwan) and kept in an animal facility for 1–2 weeks before use. All animal experimental procedures were conducted and approved by the Institutional Animal Care and Use Committee of Taipei Medical University. Five mice/group were injected subcutaneously between the scapulae with 5×10^6 of MDA-MB-231 cells. After transplantation for 1 week, mice received an i.p. injection of either 40 μl DMSO (control) or 10 mg/kg DHTS three times per week for 4 weeks. At experiment end, mice were sacrificed by cervical dislocation, and tumor specimens were taken, photographed, and weighed.

2.13. Statistical analysis

Data are presented as the mean of S.E. for the indicated number of independently performed experiments. Statistical analysis was done using one-way Student's *t*-test.

3. Results

3.1. DHTS decreased cell viability and induced G1 phase arrest in human breast adenocarcinoma cells

Two human adenocarcinoma cells, wild type p53 and estrogen-dependent MCF-7 cells and p53-mutated and estrogen-independent MDA-MB-231 cells, were used in this study. First, both cells were exposed to 0.5 μg/ml of 15,16-dihydrotanshinone I (DHTS), tanshinone I (TS), or cryptotanshinone I (CTS) for 24 h, and the cell viability was determined by MTT assay. As shown in Fig. 1B, DHTS exhibited the highest inhibitory effects on cell viability, and this was followed by TS and CTS in that order. CTS had no significant effect on cell viability under the 0.5 μg/ml concentration in either type. Base on comparisons between the chemicals structures and cytotoxicity activity, we used DHTS to examine the following experiments. Second, both cells were exposed to various concentrations of DHTS for 24 h, and the cell viability was determined by MTT assay. As shown in Fig. 1C, DHTS significantly inhibited the viability of both cell types in a dose-dependent manner, and the IC_{50} was about 0.25 μg/ml in both cells. Third, the cell cycle distributions of both cells were measured by flow cytometry after DHTS treatment. As shown in Fig. 1D, DHTS treatment retarded the progression of G1 to G2/M phase in G1-synchronous MCF-7 and MDA-MB-231 cells. In contrast, control cells successfully entered into G2/M phase release from G1-synchronous cells. These results suggest that DHTS can suppress cell proliferation and block cell cycle progression in the G1 phase.

3.2. *DHTS decreased G1 regulatory protein expression and CDK2 and CDK4 kinase activity and induced p27 expression*

To elucidate the arrest point of DHTS-treated cells in the G1 phase, we analyzed the phosphorylation state of Rb, the expression of G1 cyclins and kinases. As shown in Fig. 2A, DHTS significantly decreased the Rb phosphorylation in a dose-dependent manner in both MCF-7 and MDA-MB-231 cells. In addition, DHTS dose-dependently decreased the protein expression of PCNA, cyclin D1, cyclin D3, cyclin E, and CDK4 in both cells. On the other hand, the protein expression of total Rb, CDK2, and CDK6 in DHTS-treated cells remained unchanged. A time course experiment also showed that DHTS significantly decreased the cyclin D1 expression in the first 4 h, the cyclin D3 and cyclin E expression at 8 h, the Rb phosphorylation and CDK 4 expression at 12 h, and the PCNA expression at 16 h (Fig. 2B). To confirm DHTS can inhibit cyclin D1 gene expression, cells were transfected with cyclin D1 promoter reporter plasmid that contain 1745 bp of the cyclin D1 promoter [26] and phRL-TK plasmid as internal control. Transfected cells were treated with 0.1 μg/ml, 0.3 μg/ml, and 0.5 μg/ml DHTS for 18 h, and determined reporter luciferase activity. As shown in Fig. 2C, DHTS significantly inhibited cyclin D1 gene expression by a dose-dependent manner in MCF-7 and MDA-MB-231 cells.

To examine whether DHTS can inhibit G1 cyclin-dependent kinase activity and cause G1 arrest, we performed the CDK2 and CDK4 kinase activity assay. The kinase activities of CDK2 and CDK4 were determined after immunopreciptation from DHTS-treated cells using anti-CDK2 or anti-CDK4 antibodies and histone H1 (for CDK2) or Gst-Rb fusion protein (for CDK4) as substrates. As shown in Fig. 2D, DHTS significantly inhibited CDK2 and CDK4 kinase activities in a dose-dependent manner in both cells. To further examine whether the growth-inhibitory response to DHTS was dependent on the p53 status, and whether the inhibition of CDK2 and CDK4 were

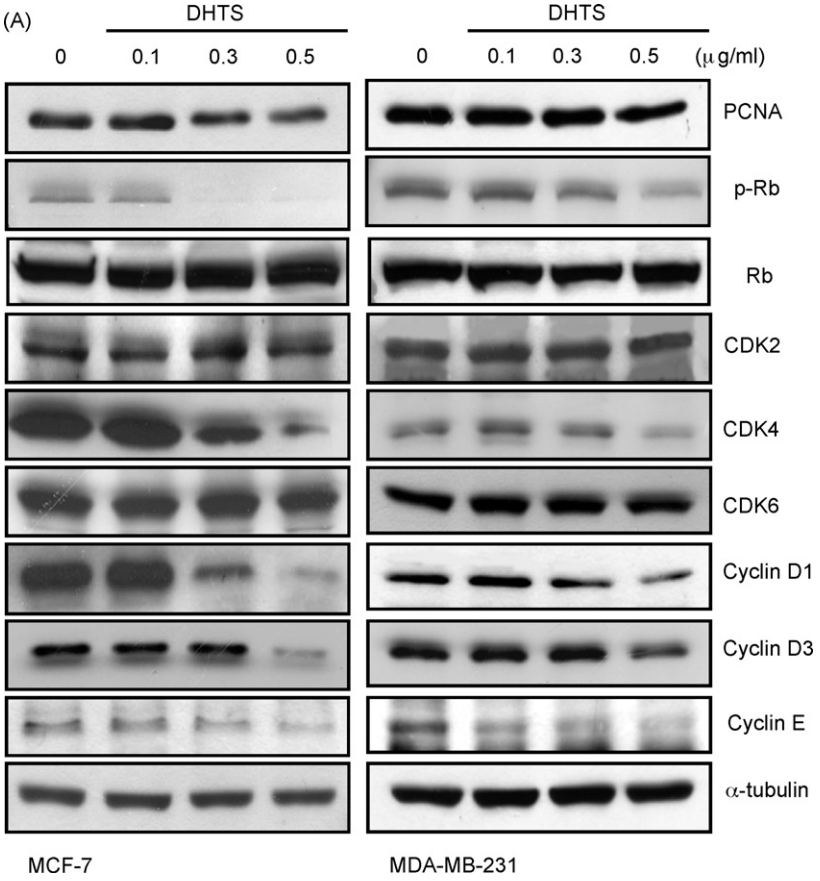

Fig. 2 – Effects of DHTS on the cell cycle arrest related protein expression and the kinase activities of CDK2 and CDK4 in breast adenocarcinoma cells. (A and C) MCF-7 cells or MDA-MB-231 cells were treated with 0.1 μg/ml, 0.3 μg/ml, or 0.5 μg/ml of DHTS for 24 h. Total cellular protein was subjected to Western blot. (B) MCF-7 cells or MDA-MB-231 cells were treated with 0.5 μg/ml of DHTS for 24 h. Total cell lysates (150 μg) were used for immunoprecipitation, the kinase activities association with the CDK2 and CDK4 immunocomplexes were assayed with histone H1 (for CDK2) or Gst-Rb (for CDK4) as substrates. The experiments were performed as described in Section 2 and ^{32}p-labeled histone H1 or Gst-Rb are shown. (D) MCF-7 cells were treated with 0.5 μg/ml of DHTS for various time points, and total cellular protein was subjected to Western blot. (E) Cells were transfected with cyclin D1 promoter reporter plasmids and phRL-TK plasmid as an internal control. After transfection, cells were treated with various concentrations of DHTS for 18 h. Cells were harvested, and the levels of luciferase activities were determined as described in Section 2. The values were obtained in three independent experiments performed in triplicate and were represented as means ± S.E. $^{*}p < 0.05$ versus control.

due to the induction of CDK inhibitors-p15, -p21, and -p27, we performed the Western blot. As shown in Fig. 2E, DHTS treatment did not change the p15 expression and significantly induced the p27 expression in both cells. Interestingly, the protein expression of p53, phosphorylated p53, and p21 decreased in DHTS-treated MCF-7 cells. However, the expression of p21 and p53 in DHTS-treated MDA-MB-231 cells showed no changes. These results suggest that the inhibitory effects of DHTS on cell progression were associated with the induction of p27 CDK inhibitor and had no relationship with the p53 status.

3.3. *DHTS induced apoptosis and decreased anti-apoptotic Bcl-xL expression*

In the following experiments, we examined whether DHTS-caused cell death was accompanied by an induction of

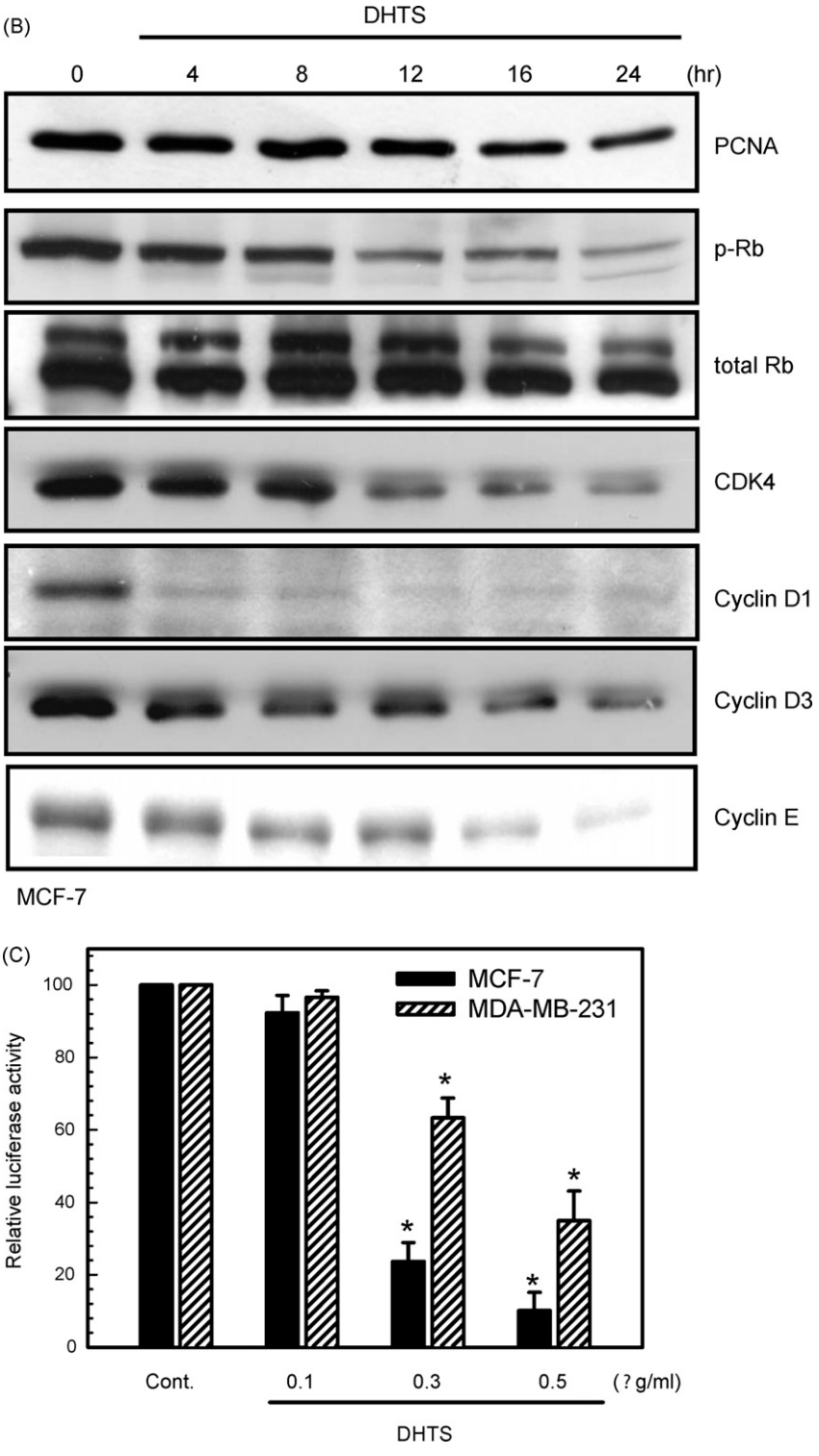

Fig. 2. (Continued)

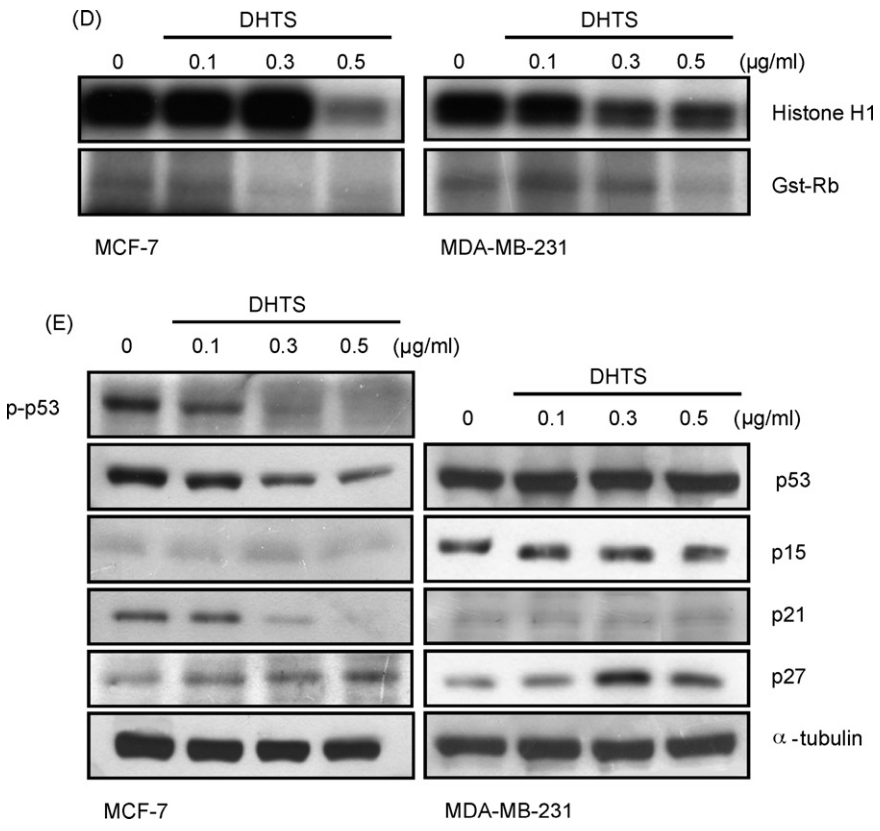

Fig. 2. (Continued).

apoptosis in MCF-7 or MDA-MB-231 cells. Both cell types were treated with 0.5 μg/ml of DHTS for 24 h and stained with PI and Annexin V-Alexa Fluor 488 followed by quantification of apoptotic cells under flow cytometry. The lower right quadrant of the FACS histogram represents the early apoptotic cells, which were stained with green fluorescence Alexa488 dye, and the upper right quadrant of FACS histogram represents the late apoptotic cells, which were stained both with red-green fluorescence PI/Alexa488 dye. As shown in Fig. 3A, we observed an increase in the early apoptotic cell population from 14.9% to 41.3% in MCF-7 cells and from 7.4% to 24.7% in MDA-MB-231 cells. We next determined the anti-apoptotic protein expression of Bcl-2 and Bcl-xL in DHTS-treated cells. After treatment of DHTS for 24 h, we found a decrease of Bcl-xL expression in both cell types, but no change in Bcl-2 expression in either type (Fig. 3B).

3.4. *DHTS induced loss of mitochondrial membrane potential and subsequently increased the release of cytochrome c*

Loss of mitochondrial membrane potential was associated with the activation of caspases and the initiation of apoptotic cascades. To examine whether DHTS induced apoptosis through the mitochondrial apoptosis pathway, MCF-7 and MDA-MB-231 cells were treated with DHTS for 24 h and the mitochondrial membrane potential was assessed by flow cytometry using the MitoProbe JC-1 assay kit. JC-1 is a cationic dye and exhibits potential-dependent accumulation in mitochondria. Under loss of mitochondrial membrane potential, the fluorescent emission of JC-1 dye shifts from red to green. Therefore, a decrease of JC-1 red fluorescence indicates a loss of mitochondrial membrane potential in cells. As shown in Fig. 3C, DHTS treatment of MCF-7 cells resulted in a decrease in red fluorescence cells from 82.2% to 67.4%, and from 79.1% to 55.5% in MDA-MB-231 cells. This suggests that DHTS treatment was able to disrupt the mitochondrial membrane potential.

Our next task was to determine whether loss of mitochondrial membrane potential could cause a cytochrome *c* release from mitochondria to cytosol. As shown in Fig. 3D, DHTS treatment indeed increased the cytosolic cytochrome *c* level but decreased the mitochondrial cytochrome *c* level.

3.5. *DHTS activated caspase-3, -7, -9 and pan-caspase inhibitor rescued DHTS-induced apoptosis*

Since cytochrome c released from mitochondria is associated with the activation of caspase-9 cascade, we next examined the activation of caspase-3, -7, and -9 in DHTS-treated breast cancer cells by Western blot detection of the cleaved caspases (active form). As shown in Fig. 4A, the cleavage of caspase-3, -7, and -9 were significantly increased in the DHTS-treated MCF-7 and MDA-MB-231 cells. In addition, we further checked the activation of caspase-3 induced by DHTS using fluorometric caspase-3 activity assay. Treatment of MCF-7 and MDA-MB-231 cells with DHTS for 24 h resulted in a significant increase in caspase-3 activity in a dose-dependent manner

(Fig. 4B). This suggests that the activation of caspase-3, -7, and -9 was a principal factor in the susceptibility of breast cancer to DHTS-induced apoptosis.

As described previously, caspase activation was involved in DHTS-induced apoptosis in MCF-7 and MDA-MB-231 cells, we next examined whether the induction of apoptosis could be reversed by pan-caspase inhibitor, z-VAD-fmk, in DHTS-treated cells. MCF-7 and MDA-MB-231 cells were pretreated with 50 μM of z-VAD-fmk for 1 h and treated with DHTS for another 24 h, before the apoptotic cells were determined as in Fig. 3A. As shown in Fig. 4C, DHTS treatment resulted in 36.6% apoptosis compared to only 14.5% in control MCF-7 cells, but apoptosis was 21.9% in the DHTS-treated cells with pan-caspase inhibitor. Similarly, DHTS-treated MDA-MB-231 cells resulted in 44.5% apoptosis, but the apoptosis fell to 28.8% with the addition of pan-caspase inhibitor.

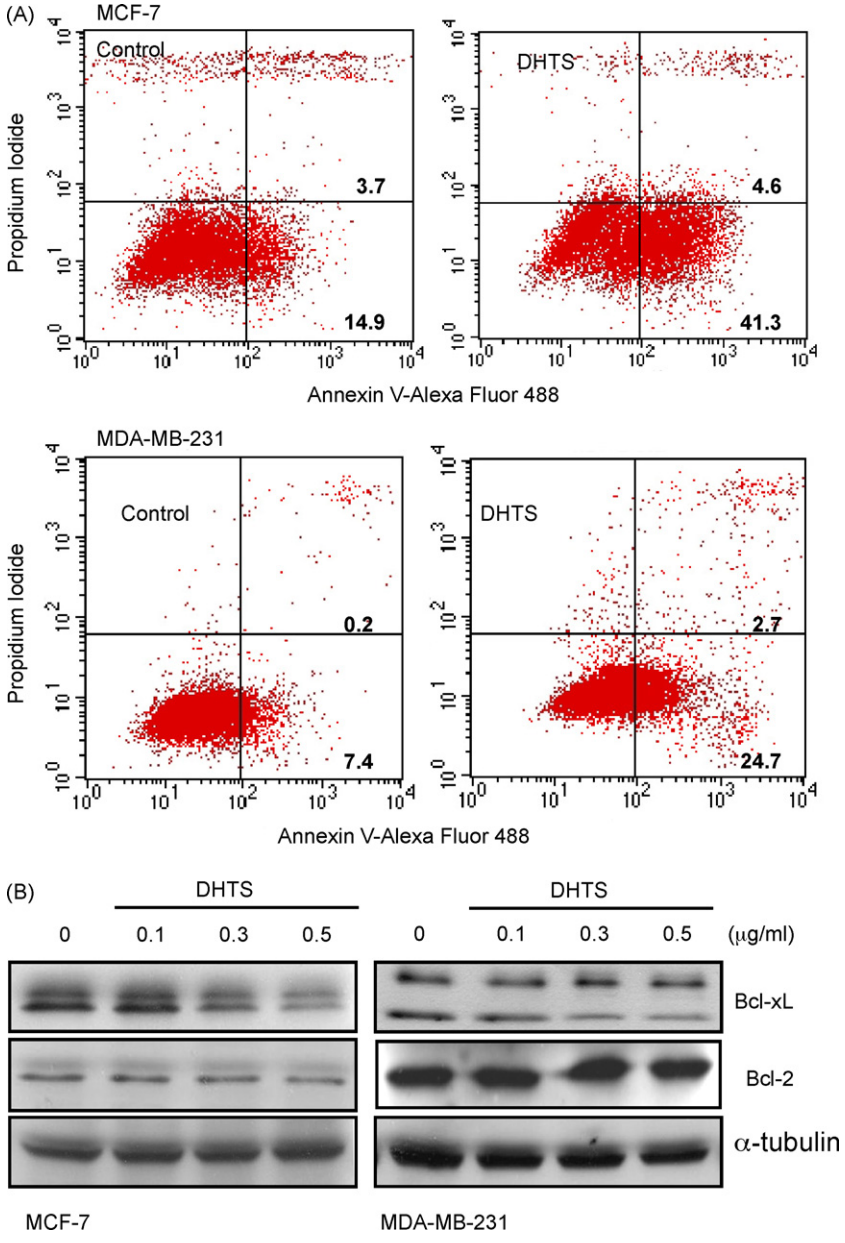

Fig. 3 – Effects of DHTS on the apoptosis, the anti-apoptotic protein expression, the loss of mitochondrial membrane potential, and the cyclochrome c release in breast adenocarcinoma cells. (A) MCF-7 cells or MDA-MB-231 cells were treated with 0.5 μg/ml of DHTS for 24 h, and the apoptotic cells were determined by FACS using the Annexin V-Alexa Fluor488 Apoptosis Assay Kit. (B) MCF-7 cells or MDA-MB-231 cells were treated with 0.5 μg/ml of DHTS for 24 h, and total cellular protein was subjected to Western blot for detection of Bcl-xL, and Bcl-2. (C) MCF-7 cells or MDA-MB-231 cells were treated with 0.5 μg/ml of DHTS for 24 h, and the membrane potential were determined by JC-1 dye probe as described in Section 2. (D) MCF-7 cells or MDA-MB-231 cells were treated with 0.5 μg/ml of DHTS for 24 h, cytosolic and mitochondrial proteins were prepared and subjected to Western blot for detection of cytochrome c. β-actin and cytochrome c oxidase (CytoOxid) were used as loading control for cytoplasmic and mitochrondrial fractions, respectively.

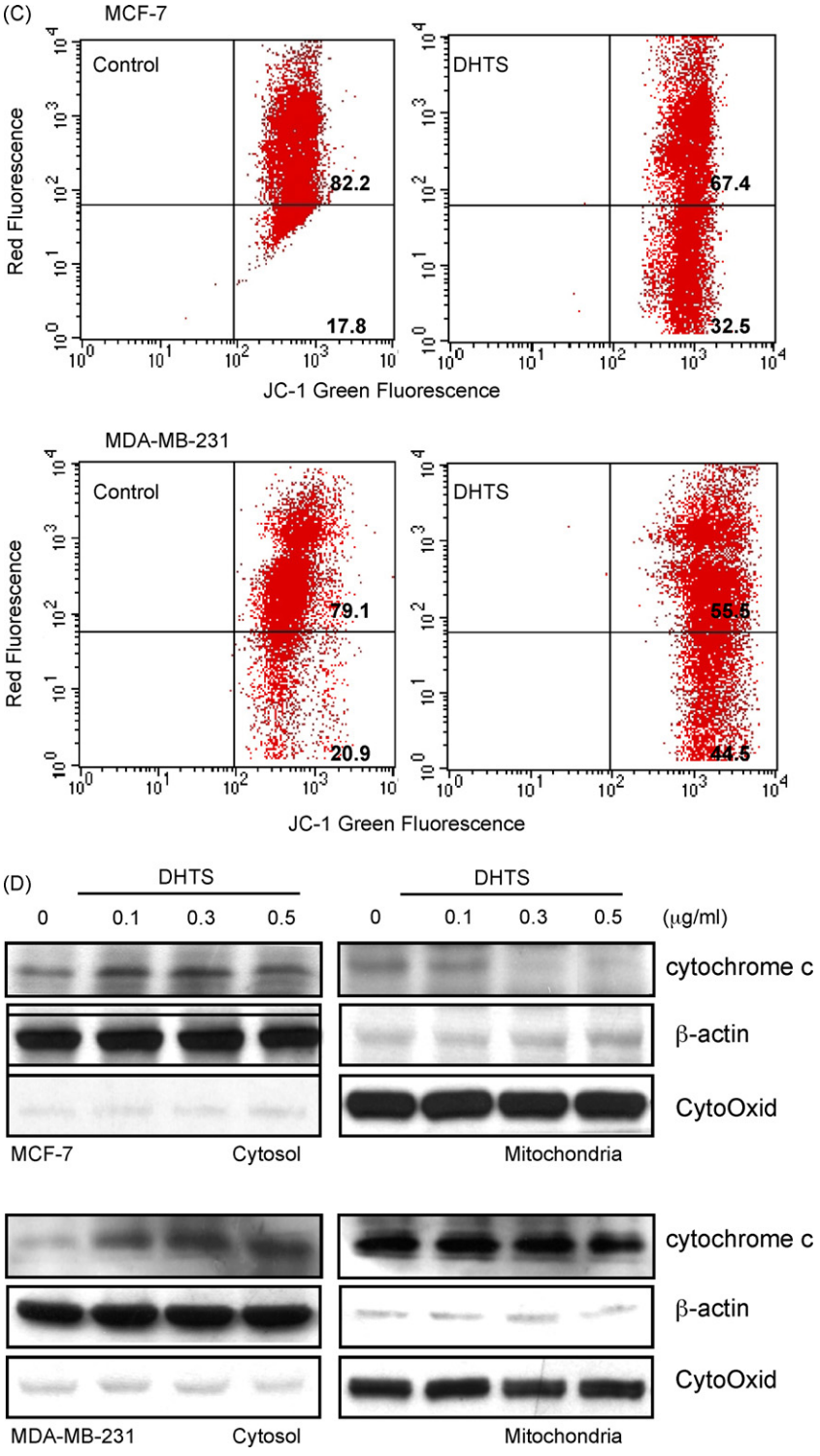

Fig. 3. (Continued).

3.6. *DHTS inhibited breast tumor growth in nude mice*

To further examine the therapeutic effect of DHTS in vivo, we treated athymic mice bearing MDA-MB-231 tumor xenografts with 10 mg/kg of DHTS for 4 weeks. At the end of the experiment, body weight and tumor weight were measured. As shown in Fig. 5, DHTS significantly inhibited tumor growth about 50% in comparison with control tumor, and body weight remained unchanged between control and DHTS-treated mice. These results suggest that DHTS not only inhibits breast adenocarcinoma proliferation in vitro but also has therapeutic activity in vivo.

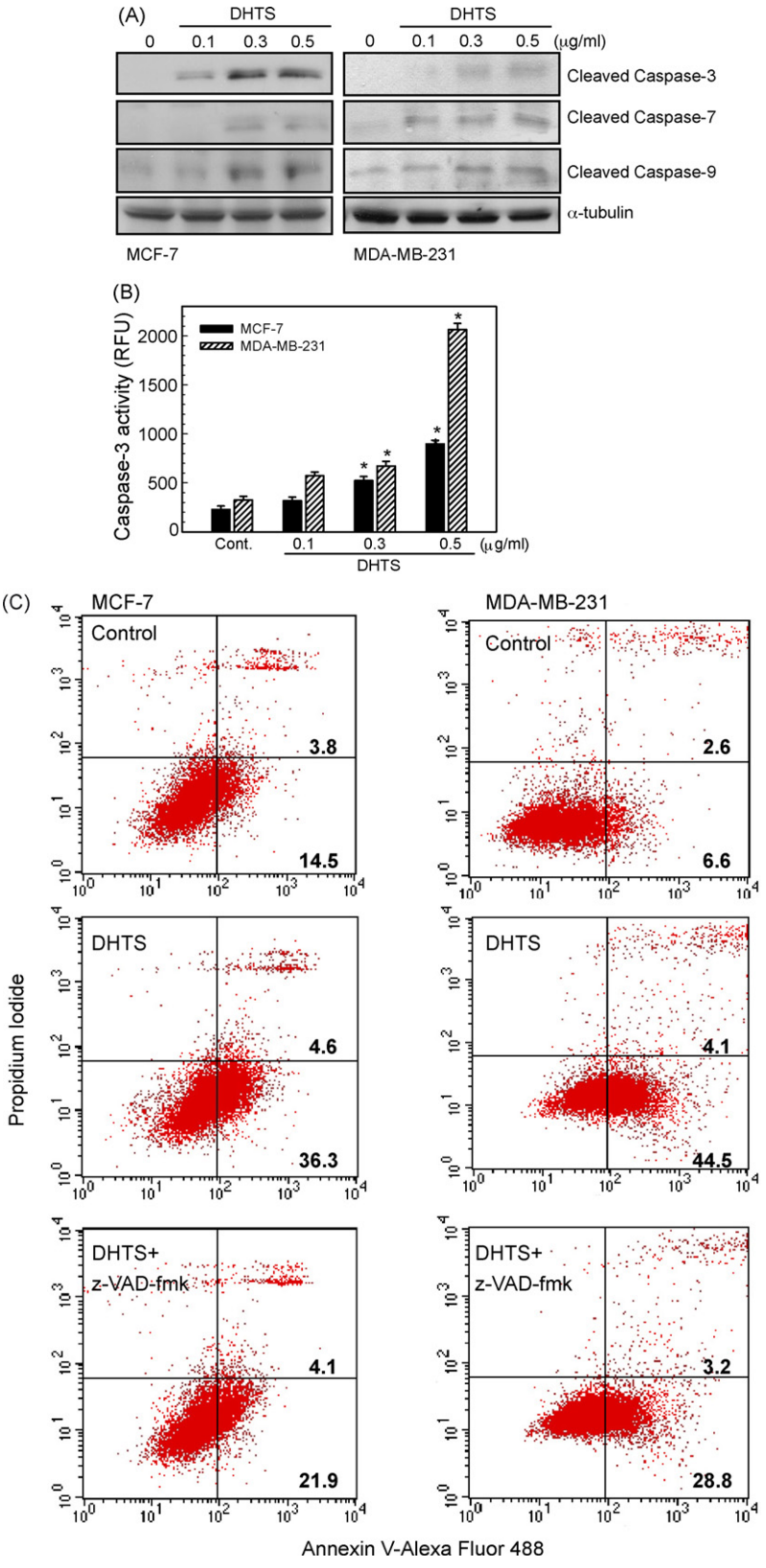

Fig. 4 – Effects of DHTS on the activation of caspase-3, caspase-7, and caspase-9 and the caspase inhibitor on the reverse of apoptosis induced by DHTS in breast adenocarcinoma cells. (A and B) MCF-7 cells or MDA-MB-231 cells were treated with 0.5 μg/ml of DHTS for 24 h, and total cell extracts were subjected to Western blot (A) and caspase-3 activity assay (B) as described in Section 2. The values were obtained in three independent experiments performed in triplicate and were represented as means ± S.E. *$p < 0.05$ versus control. (C) MCF-7 cells or MDA-MB-231 cells were pretreated with 50 μM of the pan-caspase inhibitor (z-VAD-fmk) for 1 h, and then treated with 0.5 μg/ml of DHTS for another 24 h. The apoptotic cells

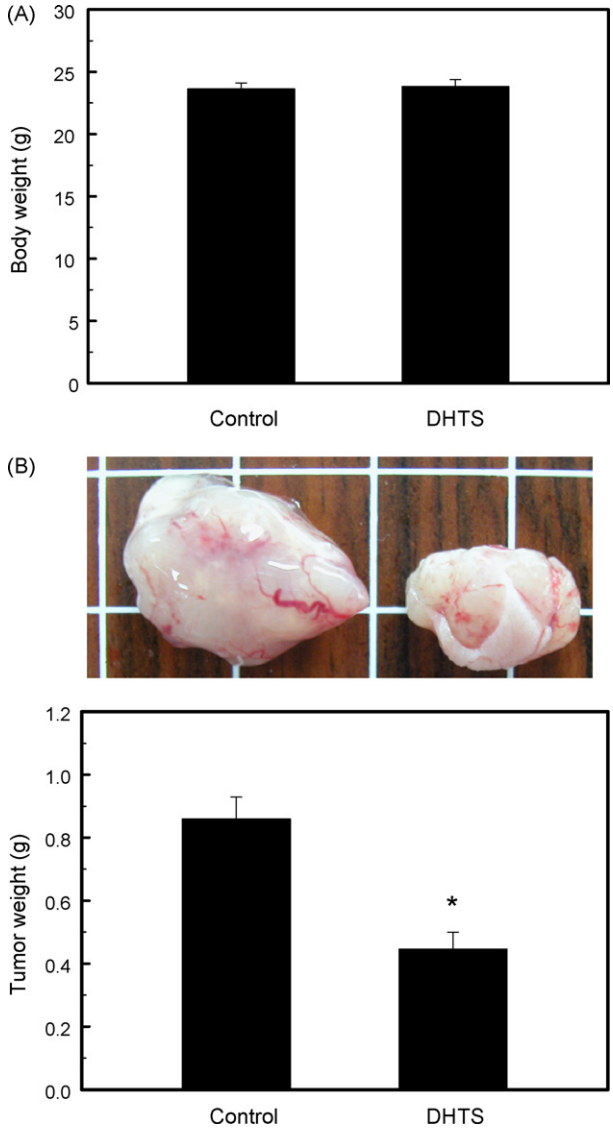

Fig. 5 – Effects of DHTS on the MDA-MB-231 tumor xenografts in nude mice. MDA-MB-231 cells were injected subcutaneously between the scapulas of athymic nude mice, and the mice were received i.p. with an injection of 10 mg/kg DHTS three times per week for 4 weeks. (A) Body weight and (B) tumor weight were measured at the end of experiment. The values were obtained in five samples and were represented as means ± S.E. *$p < 0.05$ versus control.

4. Discussion

Tanshen is widely used in Chinese traditional medicine. In this study, we evaluated DHTS, one component of Tanshen, for its activity in inhibiting the growth of human breast adenocarcinoma cells in vitro and in vivo. We observed that DHTS inhibited breast adenocarcinoma cell growth in wild type p53 and estrogen-responsive MCF-7 cells as well as p53-mutated and estrogen-independent MDA-MB-231 cells. In vitro studies showed that DHTS inhibited the proliferation of both cells through the induction of G1 phase arrest, induced apoptosis through downregulation of anti-apoptotic Bcl-xL expression, increased the loss of mitochondrial membrane potential and cytochrome *c* released, and subsequently activated the caspase-9 cascade. In vivo studies showed that intraperitoneal administration of DHTS at a dose of 10 mg/kg significantly caused a growth regression of MDA-MB-231 tumor mass. Overall, data in this present study suggest that DHTS might be a potential anti-tumor compound for breast cancer therapy.

In this study, we demonstrated that DHTS strongly inhibited breast tumor cell growth, and the inhibitory activity could be ranked as follows: DHTS > TS > CTS. This suggests that the inhibitory mechanisms of DHTS are dependent on its structure. TS showed slightly inhibitory activity than DHTS, indicating the presence of the 15,16-dihydrofuran ring has a major inhibitory effect on cell viability. CTS has a 15,16-dihydrofuran ring but showed no cytotoxic effect, indicating that the methyl benzene ring was another important structure for anti-proliferative activity in DHTS. The possible relationships between the structural properties of DHTS and anti-tumor activity deserves further investigation.

To further explore the underlying mechanisms of cell growth inhibition, we conducted a cell cycle analysis, which revealed that DHTS caused a cell cycle G1 arrest of MCF-7 and MDA-MB-231 cells released from serum-free synchronized cells (Fig. 1D). Similar to serum-free synchronized cells, DHTS blocked cell cycle progression at the G1/S boundary in aphidicolin-synchronized MCF-7 and MDA-MB-231 cells (data not shown). In addition, we synchronized cells at the G2/M boundary by treatment of cells with nocodazole, a reversible microtubule inhibitor [27]. However, DHTS also induced cell cycle G2/M arrest in nocodazole-arrested MCF-7 cells after removal of nocodazole. Previous study has demonstrated that DHTS was able to inhibit cell growth but induce cell cycle S arrest in human erythroleukemia cells K562 [22]. These results suggest that the effect of DHTS on cell cycle distribution are dependent on cell cycle states of the cultured cells and possibly cell types.

Cyclins D1, D2, and D3 belong to D-type cyclins that accumulate in the G1 phase and result in promotion of G1-S progression [28,29]. Previous studies have indicated that D-type cyclins play an important role in tumorigenesis and cyclin D1 overexpression was found in several tumor types, including breast cancer [30,31], colon cancer [32,33], thyroid cancer [34], and melanoma [35]. Interestingly, we found that DHTS significantly decreased cyclin D1 and cyclin D3 expression in breast cancer cells. DHTS could possibly inhibit tumor growths besides breast cancer.

The p27 is a member of the Cip/Kip CDK inhibitors family which acts as a negative regulator of G1-S progression by binding to cyclin E-CDK 2 complex [36]. Activated cyclin E-CDK 2 also regulates p27 expression through the phosphorylation of p27 and subsequent degradation of p27 protein through ubiquitin-mediated proteolysis [37]. In Fig. 2A, we found that cyclin E expression decreased in DHTS-treated cells, indicating a weak activation of cyclin E-CDK 2. In fact, we also found

were determined by FACS using the Annexin V-Alexa Fluor488 Apoptosis Assay Kit. The experiment was performed three times and representative data are shown.

that DHTS-treated cells had a lower CDK 2 complex kinase activity (Fig. 2D). The weak cyclin E-CDK 2 activity might lead to unphosphorylation of p27 accumulation and further promote cell cycle arrest in the G1 phase by inhibition of CDK2 kinase activity.

In conclusion, our study demonstrates that DHTS inhibits cell growth and induces the G1 arrest and apoptotic cell death of human adenocarcinoma in vitro and vivo. The inhibitory effects of DHTS were independent of functional p53 and had no relationship to estrogen responses.

Acknowledgments

This work was supported by the grant of the National Science Council, Taiwan, ROC (NSC 94-2311-B-038-002- and NSC 95-2221-E-038-011-), the Chi Mei Medical Center, Taiwan, ROC (94CM-TMU-04), and the Council of Agriculture, Executive Yuan, Taiwan, ROC (95AS-6.2.1-ST-a1).

REFERENCES

[1] Longo R, Torino F, Gasparini G. Targeted therapy of breast cancer. Curr Pharm Des 2007;13:497–517.
[2] Bremer E, van Dam G, Kroesen BJ, de Leij L, Helfrich W. Targeted induction of apoptosis for cancer therapy: current progress and prospects. Trends Mol Med 2006;12:382–93.
[3] Delivani P, Martin SJ. Mitochondrial membrane remodeling in apoptosis: an inside story. Cell Death Differ 2006;13: 2007–10.
[4] Gupta S. Molecular signaling in death receptor and mitochondrial pathways of apoptosis (Review). Int J Oncol 2003;22:15–20.
[5] Sartorius U, Schmitz I, Krammer PH. Molecular mechanisms of death-receptor-mediated apoptosis. Chembiochem 2001;8:20–9.
[6] Gupta S. Molecular steps of death receptor and mitochondrial pathways of apoptosis. Life Sci 2001;69: 2957–64.
[7] Kadowaki H, Nishitoh H, Ichijo H. Survival and apoptosis signals in ER stress: the role of protein kinases. J Chem Neuroanat 2004;28:93–100.
[8] Szegezdi E, Fitzgerald U, Samali A. Caspase-12 and ER-stress-mediated apoptosis: the story so far. Ann NY Acad Sci 2003;1010:186–94.
[9] Gogvadze V, Orrenius S, Zhivotovsky B. Multiple pathways of cytochrome c release from mitochondria in apoptosis. Biochim Biophys Acta 2006;1757:639–47.
[10] Garrido C, Galluzzi L, Brunet M, Puig PE, Didelot C, Kroemer G. Mechanisms of cytochrome c release from mitochondria. Cell Death Differ 2006;13:1423–33.
[11] Adams JM, Cory S. The Bcl-2 apoptotic switch in cancer development and therapy. Oncogene 2007;26:1324–37.
[12] van Delft MF, Huang DC. How the Bcl-2 family of proteins interact to regulate apoptosis. Cell Res 2006;16:203–13.
[13] Antignani A, Youle RJ. How do Bax and Bak lead to permeabilization of the outer mitochondrial membrane? Curr Opin Cell Biol 2006;18:685–9.
[14] Earnshaw WC, Martins LM, Kaufmann SH. Mammalian caspases: structure, activation, substrates, and functions during apoptosis. Annu Rev Biochem 1999;68:383–424.
[15] Salvesen GS. Caspases and apoptosis. Essays Biochem 2002;38:9–19.
[16] Wang X, Morris-Natschke SL, Lee KH. New developments in the chemistry and biology of the bioactive constituents of Tanshen. Med Res Rev 2007;27:133–48.
[17] Zhou L, Zuo Z, Chow MS. Danshen: an overview of its chemistry, pharmacology, pharmacokinetics, and clinical use. J Clin Pharmacol 2005;45:1345–59.
[18] Xu JK, Hiroshi K, Zheng JJ, Jiang T, Yao XS. Protective effect of tanshinones against liver injury in mice loaded with restraint stress. Yao Xue Xue Bao 2006;41:631–5.
[19] Lee P, Hur J, Lee J, Kim J, Jeong J, Kang I, et al. 15,16-Dihydrotanshinone I suppresses the activation of BV-2 cell, a murine microglia cell line, by lipopolysaccharide. Neurochem Int 2006;48:60–6.
[20] Choi HS, Cho DI, Choi HK, Im SY, Ryu SY, Kim KM. Molecular mechanisms of inhibitory activities of tanshinones on lipopolysaccharide-induced nitric oxide generation in RAW 264.7 cells. Arch Pharm Res 2004;27:1233–7.
[21] Lee SY, Choi DY, Woo ER. Inhibition of osteoclast differentiation by tanshinones from the root of *Salvia miltiorrhiza* Bunge. Arch Pharm Res 2005;28:909–13.
[22] Lee DS, Lee SH. Biological activity of dihydrotanshinone I: effect on apoptosis. J Biosci Bioeng 2000;89:292–3.
[23] Chen CH, Sheu MT, Chen TF, Wang YC, Hou WC, Liu DZ, et al. Suppression of endotoxin-induced proinflammatory responses by citrus pectin through blocking LPS signaling pathways. Biochem Pharmacol 2006;72:1001–9.
[24] Liu JD, Lin SY, Ho YS, Pan S, Hung LF, Tsai SH, et al. Involvement of c-Jun N-terminal kinase activation in 15-deoxy-Δ12,14-prostaglandin J2 and prostaglandin A1-induced apoptosis in AGS gastric epithelial cells. Mol Carcinogenesis 2003;37:16–24.
[25] Liang YC, Tsai SH, Chen L, Lin-Shiau SY, Lin JK. Resveratrol-induced G2 arrest through inhibition CDK7 and p34CDC2 kinases in colon carcinoma HT29 cells. Biochem Pharmacol 2003;65:1053–60.
[26] Guttridge DC, Albanese C, Reuther JY, Pestell RG, Baldwin Jr AS. NF-kappaB controls cell growth and differentiation through transcriptional regulation of cyclin D1. Mol Cell Biol 1999;19:5785–99.
[27] Zieve GW, Turnbull D, Mullins JM, McIntoch JR. Production of large numbers of mitotic mammalian cells by use of the reversible microtubule inhibitor nocodazole. Nocodazole accumulated mitotic cells. Exp Cell Res 1980;126:397–405.
[28] Peters G. The D-type cyclins and their role in tumorigenesis. J Cell Sci (Suppl) 1994;18:89–96.
[29] Sherr CJ. D-type cyclins. Trends Biochem Sci 1995;20:187–90.
[30] Sutherland RL, Musgrove EA. Cyclins and breast cancer. J Mammary Gland Biol Neoplasia 2004;9:95–104.
[31] Buckley MF, Sweeney KJ, Hamilton JA, Sini RL, Manning DL, Nicholson RI, et al. Expression and amplification of cyclin genes in human breast cancer. Oncogene 1993;8:2127–33.
[32] Arber N, Hibshoosh H, Moss SF, Sutter T, Zhang Y, Begg M, et al. Increased expression of cyclin D1 is an early event in multistage colorectal carcinogenesis. Gastroenterology 1996;110:669–74.
[33] Sutter T, Doi S, Carnevale KA, Arber N, Weinstein IB. Expression of cyclin D1 and E in human colon. J Med 1997;28:285–309.
[34] Baldassarre G, Belletti B, Bruni P, Boccia A, Trapasso F, Pentimalli F, et al. Overexpressed cyclin D3 contributes to retaining the growth inhibitor p27 in the cytoplasm of thyroid tumor cells. J Clin Investig 1999;104:865–74.
[35] Bosserhoff AK. Novel biomarkers in malignant melanoma. Clin Chim Acta 2006;367:28–35.
[36] Harper JW. Protein destruction: adapting roles for Cks proteins. Curr Biol 2001;11:R431–5.
[37] Johnson DG, Walker CL. Cyclins and cell cycle checkpoints. Annu Rev Pharmacol Toxicol 1999;39:295–312.